

Stable and oscillating solitons of \mathcal{PT} -symmetric couplers with gain and loss in fractional dimension

Liangwei Zeng,^{1,2} Jincheng Shi,³ Xiaowei Lu,^{1,2,*} Yi Cai,^{1,2}
Qifan Zhu,^{1,2} Hongyi Chen,^{1,2} Hu Long,^{1,2} and Jingzhen Li^{1,2,†}

¹*College of Physics and Optoelectronic Engineering, Shenzhen University, Shenzhen 518060, China*

²*Shenzhen Key Laboratory of Micro-Nano Photonic Information Technology,*

College of Physics and Optoelectronic Engineering, Shenzhen University, Shenzhen 518060, China

³*State Key Laboratory of Transient Optics and Photonics,*

Xi'an Institute of Optics and Precision Mechanics of Chinese Academy of Sciences, Xi'an 710119, China

Families of coupled solitons of \mathcal{PT} -symmetric physical models with gain and loss in fractional dimension and in settings with and without cross-interactions modulation (CIM), are reported. Profiles, powers, stability areas, and propagation dynamics of the obtained \mathcal{PT} -symmetric coupled solitons are investigated. By comparing the results of the models with and without CIM, we find that the stability area of the model with CIM is much broader than the one without CIM. Remarkably, oscillating \mathcal{PT} -symmetric coupled solitons can also exist in the model of CIM with the same coefficients of the self- and cross-interactions modulations. In addition, the period of these oscillating coupled solitons can be controlled by the linear coupling coefficient.

I. INTRODUCTION

The nonlinear Schrödinger equation (NLSE) [1–10], which can be used to describe the dynamics of optical solitons in laser beam or matter-wave solitons in Bose-Einstein condensate (BEC), has drawn more and more attention in recent decades. It is also widely used in quantum mechanics [11], hydrodynamics [12], nonlinear optics [3, 7], BEC [3, 7] as well as superconductivity [13]. Note that it is easy to stabilize a one-dimensional soliton, since it is now widely known that the bright soliton is the exact solution of one-dimensional NLSE with uniform cubic self-focusing nonlinearity. However, the collapse will happen in two-dimensional NLSE with uniform cubic self-focusing nonlinearity [14]. A popular way to avoid such collapse is the introduction of the linear potentials [15–17], which can stabilize various kinds of solitons in all dimensions. Another way to create stable solitons in high dimensions is the introduction of nonlinearities, such as the employment of periodically modulated nonlinearities [3, 18, 19] or spatially inhomogeneous defocusing nonlinearities [20–24].

It is worth to mention that single NLSE can only describe the propagation of an optical soliton in a laser beam or the evolution of a matter-wave soliton in a BEC. As for the settings of two (or more) laser beams or BECs, the models of coupled NLSEs [25–31] have to be considered due to the coupled interactions of the laser beams or BECs. These models are widely studied in optical couplers, especially in the fields of optical fiber [32, 33] and waveguide [34] in recent years. Further, the models of couplers with parity-time- (\mathcal{PT} -) symmetry have drawn more and more attention, since Bender demonstrated that non-Hermitian Hamiltonians with \mathcal{PT} -symmetry

can have real spectra [35], which is an important extension of standard quantum mechanics. These physical models with \mathcal{PT} -symmetry exhibit some novel physical properties due to their non-Hermitian Hamiltonians [36, 37] and various physical settings with \mathcal{PT} -symmetry have been widely investigated during the past decade [38–44].

The fractional derivative [45], firstly introduced by Laskin, is another great extension of the standard quantum mechanics [46–48]. Under such condition, the quantum mechanics becomes the fractional quantum mechanics, and the NLSE becomes the nonlinear fractional Schrödinger equation (NLFSE). Followed by the above landmark study of Laskin in the NLSE, various studies have been reported in recent years [49–81], including the propagation of light beams [51, 52], accessible solitons [55, 56], gap solitons [57, 67], vortex solitons [69, 72, 80], solitons in nonlinear lattices [64], and soliton clusters [70, 71].

Despite so many researches that have been reported in the NLFSE, the coupled \mathcal{PT} -symmetric NLFSEs with gain and loss, which can be used to describe the propagations of binary \mathcal{PT} -symmetric laser beams or BECs with coupled interactions, have not been yet reported, to the best of our knowledge. This coupled model can be employed to study the optical waveguides and fiber couplers, which have great potential in optical communications. The objective of this work is to extend the NLFSE to its coupled form with \mathcal{PT} -symmetry, from which we can explore the existence, stability and other properties of optical and matter-wave solitons in this model under fractional-order diffraction.

This paper is organized as follows. In Sec. II, we introduce the theoretical model and report some typical analytical solutions for coupled solitons. Sec. III, which presents numerical results for \mathcal{PT} -symmetric coupled solitons, is divided into two parts. The numerical results for the model without cross-interactions modu-

* xiaoweilu@szu.edu.cn

† lijz@szu.edu.cn

lations are given in Sec. III A, and the corresponding numerical results for the model with cross-interactions modulations are reported in Sec. III B. We find that the field profiles and stability domains of coupled solitons are strongly affected by the linear coupling coefficient, the fractional-order diffraction described by the Lévy index α , the propagation constant, and the cross-interactions modulation. It should be mentioned that these coupled solitons can exist only when the gain/loss parameter (γ) is less than the linear coupling coefficient (κ). Finally, the paper is summarized in Sec. IV.

II. THEORETICAL MODEL

The propagations of laser beams in \mathcal{PT} -symmetric couplers with gain and loss under fractional-order diffraction can be described by the dimensionless coupled NLFSEs

$$\begin{cases} i\frac{\partial U_1}{\partial z} = \frac{1}{2} \left(-\frac{\partial^2}{\partial x^2} \right)^{\alpha/2} U_1 - g|U_1|^2 U_1 - \epsilon|U_2|^2 U_1 \\ \quad - \kappa U_2 + i\gamma U_1, \\ i\frac{\partial U_2}{\partial z} = \frac{1}{2} \left(-\frac{\partial^2}{\partial x^2} \right)^{\alpha/2} U_2 - g|U_2|^2 U_2 - \epsilon|U_1|^2 U_2 \\ \quad - \kappa U_1 - i\gamma U_2. \end{cases} \quad (1)$$

Here $U_{1,2}$ and z represent the field amplitudes and propagation distance, respectively, $g > 0$ and $\epsilon > 0$ represent the coefficients of attractive self- and cross-interactions modulations of the components, respectively. Note that $g < 0$ and $\epsilon < 0$ denote the coefficients of repulsive self- and cross-interactions modulations of the components that can be used to generate dark solitons [82]. In this article, we focus on the formation of bright solitons, hence the case when $g < 0$ and $\epsilon < 0$ is not discussed here. The parameter $\kappa > 0$ denotes the linear coupling coefficient, and $\gamma > 0$, that is the coefficient of gain and loss, stands for the gain in one component and the loss in the other one. Note that $(-\partial^2/\partial x^2)^{\alpha/2}$ denotes the fractional derivative, where α ($1 < \alpha \leq 2$) stands for the Lévy index. The definition of fractional derivative is as follows [46–48]

$$\begin{aligned} \left(-\frac{\partial^2}{\partial x^2} \right)^{\alpha/2} U &= \frac{1}{2\pi} \int_{-\infty}^{+\infty} |s|^\alpha ds \\ &\times \int_{-\infty}^{+\infty} d\zeta \exp[ip(x-\zeta)] U(\zeta). \end{aligned} \quad (2)$$

In particular, Eqs. (1) will degenerate to the generic \mathcal{PT} -symmetric coupled nonlinear Schrödinger equations when $\alpha = 2$. As for BECs, $U_{1,2}$ and z should be replaced by the wave functions $\phi_{1,2}$ and time t .

With the real propagation constant b (b should be replaced by chemical potential $-\mu$ in BECs), the stationary solutions of these \mathcal{PT} -symmetric coupled solitons with

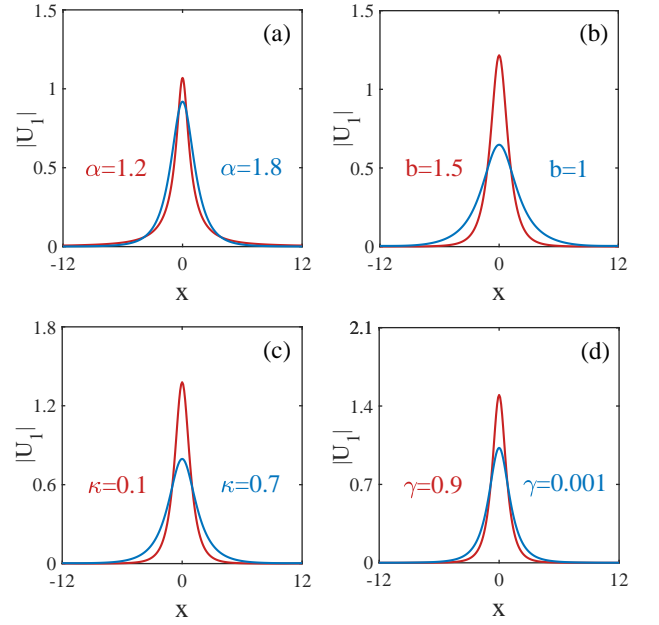


FIG. 1. Profiles of solitons (shown for components of U_1): (a) with different values of α at $\kappa = 0.8$, $\gamma = 0.001$, $b = 1.2$; (b) with different values of b at $\alpha = 1.8$, $\kappa = 0.8$, $\gamma = 0.001$; (c) with different values of κ at $\alpha = 1.8$, $\gamma = 0.001$, $b = 1$; (d) with different values of γ at $\alpha = 1.8$, $\kappa = 1$, $b = 1.5$. The profiles of $|U_2|$ are similar to $|U_1|$. $\epsilon = 0$ are used in Figs. 1~3. $g = 1$ are used throughout this paper.

gain and loss can be found by generic forms

$$\begin{cases} U_1(x, z) = U(x)\exp(ibz - i\delta/2), \\ U_2(x, z) = U(x)\exp(ibz + i\delta/2). \end{cases} \quad (3)$$

Here δ denotes the constant phase shift between the components, which is given by

$$\delta = \arcsin(\gamma/\kappa). \quad (4)$$

As is seen from Eqs. (3) and (4), the difference between the two components $U_{1,2}$, which is caused by their parameter of gain-loss, is their imaginary part $\exp(\pm i\delta/2)$. Due to their opposite parameter of gain-loss, these two components will have the opposite transition of energy in their propagations, which can be referred to the following Figs. 3, 6, 7, 8 and 9.

Here the real function $U(x)$ satisfies the generic stationary NLFSE with a varying value of the propagation constant b

$$-(b - \kappa_s)U = \frac{1}{2} \left(-\frac{\partial^2}{\partial x^2} \right)^{\alpha/2} U - gU^3 - \epsilon U^3, \quad (5)$$

$$\kappa_s = \sqrt{\kappa^2 - \gamma^2}. \quad (6)$$

According to Eq. (6), it is easy to see that these coupled solitons can exist only when

$$\gamma \leq \gamma_{max} = \kappa. \quad (7)$$

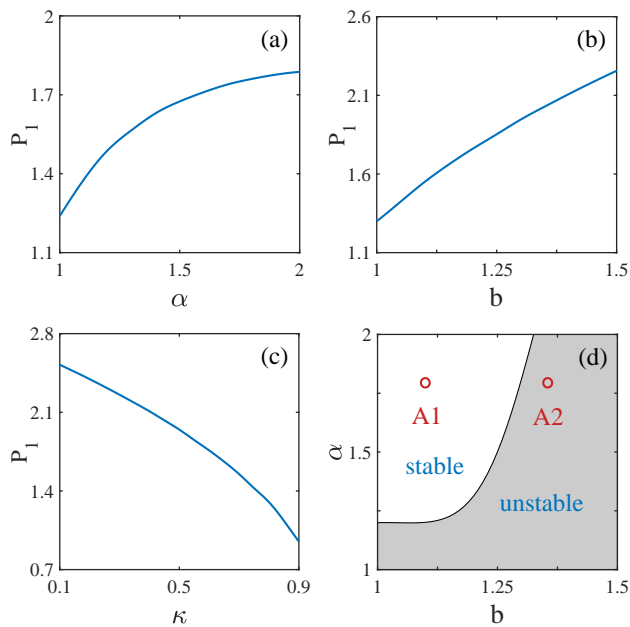


FIG. 2. (a) Soliton power P versus α at $\kappa = 0.8$, $\gamma = 0.001$, $b = 1.2$. (b) P versus b at $\alpha = 1.8$, $\kappa = 0.8$, $\gamma = 0.001$. (c) P versus κ at $\alpha = 1.8$, $\gamma = 0.001$, $b = 1$. (d) Stability (white) and instability (gray) domains for the coupled solitons with $\kappa = 0.8$, $\gamma = 0.001$ in the (b, α) plane. The propagations of the solitons corresponding to the points marked by A1 and A2 are shown in Figs. 3(a,b) and 3(c,d), respectively.

From Eq. (7), the largest value of the gain-loss coefficient in these \mathcal{PT} -symmetric couplers is limited to the value of the linear coupling coefficient κ .

Particularly, analytical solution of Eq. (5) can be solved when $\alpha = 2$, which is given by

$$U = \sqrt{2(b - \kappa_s)/(g + \epsilon)} \operatorname{sech} \left(\sqrt{2(b - \kappa_s)} x \right), \quad (8)$$

where κ_s is defined by Eq. (6).

The soliton power P of $U_{1,2}$ is defined by $P_1 = \int |U_1|^2 dx$, $P_2 = \int |U_2|^2 dx$. In this paper, the modified squared-operator method [83] and split-step Fourier method are employed to solve the stationary solutions for Eq. (5) and numerical simulations for Eqs. (1) respectively.

III. NUMERICAL RESULTS

In this section, we focus on presenting our numerical results of \mathcal{PT} -symmetric coupled solitons with gain and loss under different parameters in the models of Eqs. (1) and Eq. (5), including the \mathcal{PT} -symmetric coupled solitons with different linear coupling coefficients, fractional-order diffractions, propagation constants and cross-interactions modulations. Particularly, we find that the cross-interactions modulation can greatly affect these

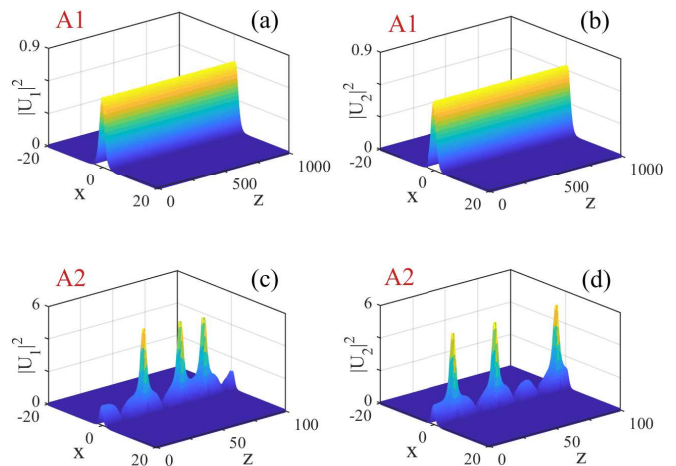


FIG. 3. Propagations of coupled solitons with different values of b at $\alpha = 1.8$, $\kappa = 0.8$, $\gamma = 0.001$: (a,b) with $b = 1$; (c,d) with $b = 1.35$. The left / right column displays the U_1 / U_2 component.

coupled solitons. Thus we divide our numerical results into two parts, namely the coupled solitons without/with cross-interactions modulations which can be referred to Sec. III A and Sec. III B, respectively.

A. Coupled solitons without cross-interactions modulation

The \mathcal{PT} -symmetric physical model without cross-interactions modulation means that the coefficient $\epsilon = 0$, which is a simple model but a nontrivial one. We now display the relevant numerical results in this setting. Note that the numerical results under this setting are shown in Figs. 1~3. According to Eq. (6), it is not difficult to find that these real \mathcal{PT} -symmetric coupled solutions can only be supported under the condition of $\gamma \leq \kappa$. For simplicity, note also that we use $g = 1$ throughout this article. Profiles of the \mathcal{PT} -symmetric coupled solitons with different values of the Lévy index α , different propagation constants b , different linear coupling coefficients κ , and different values of the gain and loss parameter γ are shown in Figs. 1(a~d), respectively. According to Eqs. (3), we see that the stationary solutions of solitons $U_1(x)$ and $U_2(x)$ have the same real part $U(x)$ and conjugate imaginary parts $\exp(\pm i\delta/2)$, that is, $U_1(x) = U(x)\exp(-i\delta/2)$, $U_2(x) = U(x)\exp(i\delta/2)$. Note also that the propagation constant b will disappear in the expressions of the stationary solutions of solitons $U_1(x)$ and $U_2(x)$ after we submit Eqs. (3) into Eqs. (1). According to the above expressions of $U_1(x)$ and $U_2(x)$, the profiles of the modulus $|U_2|$ are similar to those of the modulus $|U_1|$, thus we display here only the profiles of $|U_1|$. From Fig. 1(a), the amplitude of coupled solitons decreases and the width increases when α increases. Ac-

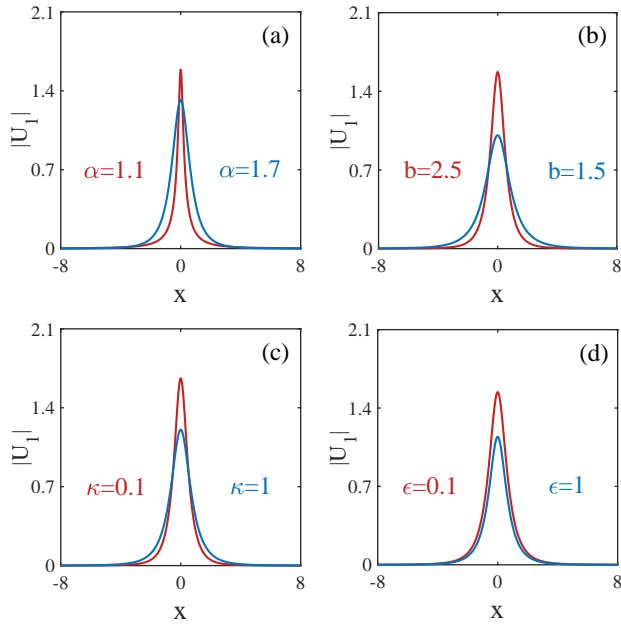


FIG. 4. Profiles of solitons (shown for components of U_1): (a) with different values of α at $\kappa = 0.8$, $\epsilon = 0.5$, $\gamma = 0.001$, $b = 2$; (b) with different values of b at $\alpha = 1.7$, $\kappa = 0.8$, $\epsilon = 0.5$, $\gamma = 0.001$; (c) with different values of κ at $\alpha = 1.7$, $\epsilon = 0.5$, $\gamma = 0.001$, $b = 2$; (d) with different values of ϵ at $\alpha = 1.7$, $\kappa = 0.8$, $\gamma = 0.001$, $b = 2$. The profiles of $|U_2|$ are similar to $|U_1|$.

According to Fig. 1(b), the amplitude of coupled solitons increases and the width decreases when b increases. Note also that the amplitude of coupled solitons decreases and the width increases when κ increases, as presented in Fig. 1(c), similar to the situation in Fig. 1(a). In Fig. 1(d), the amplitude of coupled solitons increases with the increase of γ and the width of solitons decreases with the increase of γ .

We now focus on the soliton power of the obtained families of coupled solitons, including the relationships of the soliton power P versus the Lévy index α , P versus the propagation constant b , and P versus the linear coupling coefficient κ . We point out that the dependences of the soliton power of the $|U_2|$ component on the parameters of the model are similar to those of the $|U_1|$ component. Fig. 2(a) shows that the soliton power P_1 increases with the increase of α , and the increasing speed gradually decreases. According to Fig. 2(b), the soliton power increases when b increases, which shows that the relationship between soliton power and propagation constant satisfies the Vakhitov-Kolokolov (VK) stability criterion $\partial P/\partial b > 0$, which is a necessary but not sufficient condition for stable soliton solutions [84]. The soliton power decreases with the increase of κ , as presented in Fig. 2(c). The stable and unstable domains of these \mathcal{PT} -symmetric coupled solitons are very important, here, Fig. 2(d) displays the stability (white) and

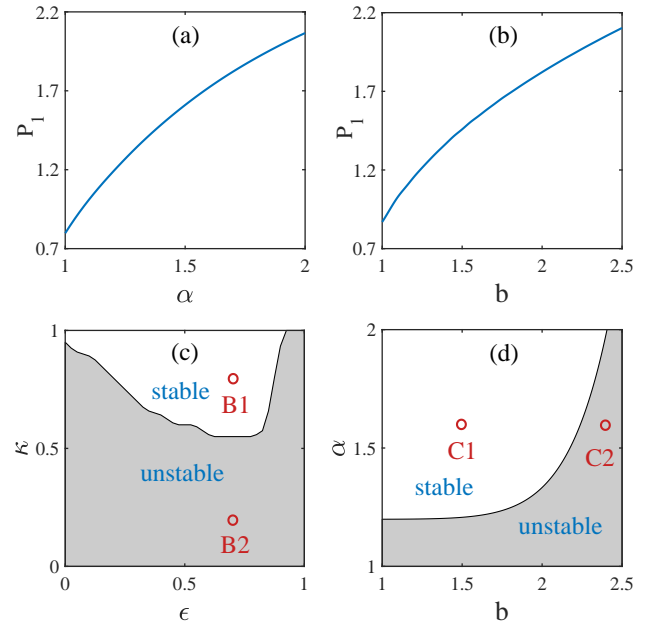


FIG. 5. (a) P versus α at $\kappa = 0.8$, $\epsilon = 0.5$, $\gamma = 0.001$, $b = 2$. (b) P versus b at $\alpha = 1.7$, $\kappa = 0.8$, $\epsilon = 0.5$, $\gamma = 0.001$. (c) Stability (white) and instability (gray) domains for the coupled solitons with $\alpha = 1.7$, $\gamma = 0.001$, $b = 1.5$ in the (ϵ, κ) plane. The propagations of the solitons corresponding to the points marked by B1 and B2 are shown in Figs. 6(a,b) and 6(c,d), respectively. (d) Stability (white) and instability (gray) domains for the coupled solitons with $\kappa = 0.8$, $\epsilon = 0.5$, $\gamma = 0.001$ in the (b, α) plane. The propagations of the solitons corresponding to the points marked by C1 and C2 are displayed in Figs. 7(a,b) and 7(c,d), respectively.

instability (gray) domains for the obtained coupled solitons in the (b, α) plane. From Fig. 2(d), we can find that the coupled solitons can be stable only when the Lévy index $\alpha \geq 1.2$. The propagation dynamics of the coupled solitons marked by the points A1 and A2 are presented in Figs. 3(a,b) and 3(c,d), respectively. The coupled solitons marked by the point A1 are stable, and both components of the coupled solitons are keeping their amplitudes and shapes even after a long propagation distance (propagation distance $z = 1000$), as displayed in Figs. 3(a,b). On the other hand, the coupled solitons marked by the point A2 are unstable, and both components of the coupled solitons are greatly distorted after some propagation distance, as presented in Figs. 3(c,d).

B. Coupled solitons with cross-interactions modulation

In this subsection, we focus on coupled solitons with cross-interactions modulation, that is, when $\epsilon > 0$). It should be mentioned that the numerical results under this setting are displayed in Figs. 4~9. Fig. 4 shows the profiles of \mathcal{PT} -symmetric coupled solitons with different

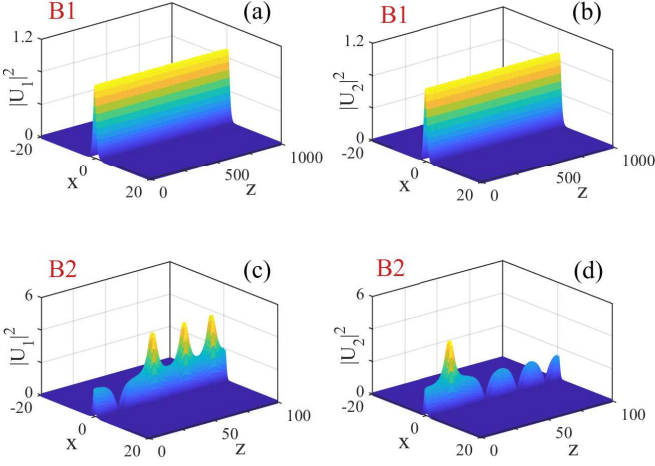


FIG. 6. Propagations of coupled solitons with different values of κ at $\alpha = 1.7$, $\epsilon = 0.7$, $\gamma = 0.001$, $b = 1.5$: (a,b) with $\kappa = 0.8$; (c,d) with $\kappa = 0.2$. The left / right column displays the U_1 / U_2 component.

parameters, including the solitons with different Lévy indices α , different propagation constants b , different linear coupling coefficients κ , and different cross-interactions modulations ϵ . The profiles of $|U_2|$ are similar to $|U_1|$, therefore, we only display the profiles of $|U_1|$ in this subsection.

The amplitude of coupled solitons decreases and the width of increases when α increases, as shown in Fig. 4(a). In Fig. 4(b), the amplitude of coupled solitons increases while the width decreases with the increase of b . According to Fig. 4(c), the amplitude of coupled solitons decreases and the width increases when κ increases. From Fig. 4(d), the amplitude and width of coupled solitons increase when ϵ increases. Obviously, the results shown in Figs. 4(a~c) are similar to their counterparts shown in Figs. 1(a~c) (without cross-interactions modulation).

Fig. 5 displays the soliton power and relevant stability area of these \mathcal{PT} -symmetric coupled solitons with cross-interactions modulation. Here, the soliton power of $|U_2|$ is similar to that of $|U_1|$. Fig. 5(a) demonstrates that the soliton power P_1 increases with the increase of α , and the growth speed gradually diminishes. From Fig. 5(b), the soliton power increases when b increases, which demonstrates that the relationship between soliton power and propagation constant for the obtained coupled solitons also satisfies the VK stability criterion. The stable and unstable domains of the coupled solitons with cross-interactions modulation are also very important. Here, Figs. 5(c,d) show the stability (white) and instability (gray) domains for the coupled solitons in the (ϵ, κ) and (b, α) planes, respectively. According to Fig. 5(c), the coupled solitons can be stable only when κ is above a certain threshold, which is about 0.55 in this case. Fig. 5(d) demonstrates that these coupled solitons can be stable only when $\alpha \geq 1.2$. Further, by comparing the results

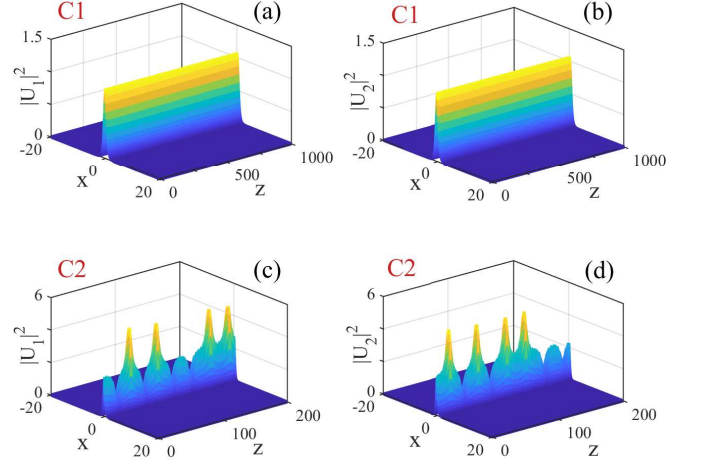


FIG. 7. Propagations of coupled solitons with different values of b at $\alpha = 1.6$, $\kappa = 0.8$, $\epsilon = 0.5$, $\gamma = 0.001$: (a,b) with $b = 1.5$; (c,d) with $b = 2.4$. The left / right column displays the U_1 / U_2 component.

of Fig. 5(d) and Fig. 2(d), we can clearly see that the stable domain of Fig. 5(d) is much broader than the one in Fig. 2(d). Note that other parameters in Fig. 5(d) and Fig. 2(d) are the same except for cross-interactions modulation ϵ , therefore, we can draw a conclusion that ϵ can greatly affect the stability and instability domains.

The propagation dynamics of the coupled solitons marked by the points (B1,B2) [in Fig. 5(c)] and (C1,C2) [in Fig. 5(d)] are presented in Figs. 6 and 7, respectively. The coupled solitons marked by the points B1 and C1 are stable, and both components of these coupled solitons are keeping their amplitudes and shapes even after long-distance propagations (after a propagation distance $z = 1000$), as displayed in Figs. 6(a,b) and 7(a,b). On the other hand, the coupled solitons marked by the points B2 and C2 are unstable, and both components of these coupled solitons are greatly distorted even after short-distance propagations, as presented in Figs. 6(c,d) and 7(c,d).

Next we turn to investigate the formation and propagation properties of the oscillating \mathcal{PT} -symmetric coupled solitons in the model of cross-interactions modulation. It was mentioned before that $g = 1$ is used throughout this paper; here we find that the unstable coupled solitons become oscillating coupled solitons when $\epsilon = 1$. Some examples of the oscillating coupled solitons are displayed in Fig. 8, which shows the propagation dynamics of U_1 in the left column and the corresponding propagation dynamics of U_2 in the right column. Figs. 8(a,b) display the propagation dynamics of the oscillating coupled solitons with a long oscillating period, and Figs. 8(c~f) present the propagation dynamics of the oscillating coupled solitons with a short oscillating period. According to Figs. 8(a,b), we see that when the amplitude of one component decreases, the amplitude of the other compo-

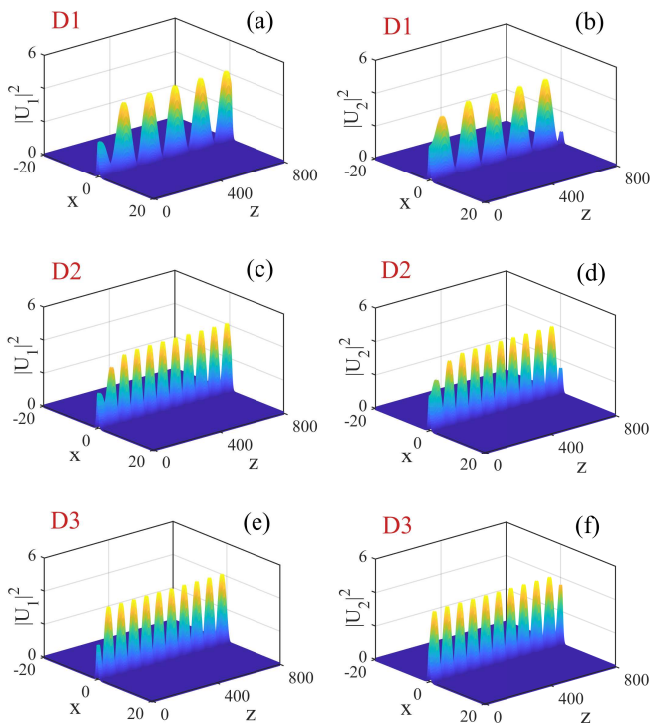


FIG. 8. Stable propagations of oscillating solitons at $\alpha = 1.8$, $\epsilon = 1$, $b = 2$: (a,b) with $\kappa = 0.02$, $\gamma = 0.01$; (c,d) with $\kappa = 0.04$, $\gamma = 0.01$; (e,f) with $\kappa = 0.04$, $\gamma = 0.038$. The left / right column displays the U_1 / U_2 component. Note that the oscillating period can be controlled only by varying the value of κ . The soliton power P versus propagation distance z for panels (a)~(c) are displayed in Figs. 9(a)~9(c), respectively.

ment would increase at the same time, which is related to the coefficient of gain and loss γ .

To further study the properties of these interesting oscillating \mathcal{PT} -symmetric coupled solitons, we draw the relationships between their soliton power P and propagation distance z in Fig. 9 (whose propagation dynamics are presented in Fig. 8). In Fig. 9, the yellow and blue lines stand for P_1 and P_2 , respectively. By comparing the results in Figs. 9(a,b), we can see that the oscillating period depends on the linear coupling coefficient κ , and it decreases when κ increases. In addition, we point out that the convergence speed of transforming the coupled solitons into oscillating coupled solitons is strongly related to the specific value of the gain/loss parameter γ . That is to say, the larger γ is, the faster the coupled solitons transform into the oscillating coupled solitons. It should be emphasized that we have verified the above conclusions by using different sets of parameters. Furthermore, we find that these oscillating \mathcal{PT} -symmetric coupled solitons can be supported under the condition of $g = \epsilon > 0$, which is not limited to $g = \epsilon = 1$.

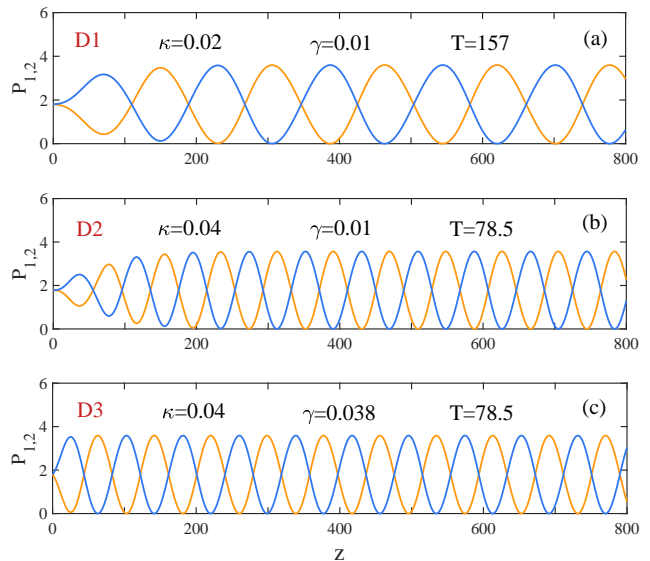


FIG. 9. Soliton power P versus z for the propagation displayed in Figs. 8(a)~8(c). The yellow and blue lines stand for P_1 and P_2 , respectively. Note that the parameter γ can not affect the oscillating period T , while it can affect the convergence speed to the equilibrium state.

IV. CONCLUSION

In this paper, we have investigated the existence and propagation dynamics of the families of coupled solitons in \mathcal{PT} -symmetric physical models with gain and loss in fractional dimension, including the coupled models with and without cross-interactions modulation. The profiles, powers, stability domains, and propagation properties of these \mathcal{PT} -symmetric coupled solitons are studied in both physical settings. According to our study, the profiles of such \mathcal{PT} -symmetric coupled solitons are sensitive to the values of propagation constant, and the stable coupled solitons can only exist under the condition that the Lévy index is greater than a critical value. In addition, the obtained results reveal that the cross-interactions modulation can greatly affect the stability and instability domains of the coupled solitons. In other words, the stability area of the model with cross-interactions modulation is much broader than the one without cross-interactions modulation. Further, we have also studied the oscillating \mathcal{PT} -symmetric coupled solitons that can be supported when the coefficients of the self- and cross-interactions modulations are the same. Besides, the oscillating period of these coupled solitons can be controlled by varying the value of the linear coupling coefficient, and the convergence speed of coupled solitons that are transforming into oscillating coupled solitons is only related to the value of the gain/loss parameter.

The physical model studied in this work can be extended to the (2+1)-dimensional setting, which is an interesting but a quite difficult problem due to the presence

of the critical collapse [14]. Also, the introduction of linear periodic potentials into the physical model is another interesting issue to be investigated, because the coupled gap solitons [85] can form in that setting.

ACKNOWLEDGMENT

We thank Dumitru Mihalache and Jiawei Li for their help on improving the writing of the manuscript.

FUNDING

This work was supported by National Major Instruments and Equipment Development Project of National

Natural Science Foundation of China (No. 61827815), by National Natural Science Foundation of China (No. 62075138), and by Science and Technology Project of Shenzhen (Nos. JCYJ20190808121817100, JCYJ20190808164007485).

CONFLICT OF INTEREST

The authors declare that they have no conflict of interest.

-
- [1] Hasegawa, A., Kodama, Y.: Solitons in Optical Communications. Oxford University Press, Oxford (1995)
- [2] Serkin, V.N., Hasegawa, A.: Novel Soliton Solutions of the Nonlinear Schrödinger Equation Model. *Phys. Rev. Lett.* **85**, 4502-4505 (2000)
- [3] Kartashov, Y.V., Malomed, B.A., Torner, L.: Solitons in nonlinear lattices. *Rev. Mod. Phys.* **83**, 247-305 (2011)
- [4] Wang, L., Porsezian, K., He, J.: Breather and rogue wave solutions of a generalized nonlinear Schrödinger equation. *Phys. Rev. E* **87**, 053202 (2013)
- [5] Chiu, T.L., Liu, T.Y., Chan, H.N., Chow, K.W.: The dynamics and evolution of poles and rogue waves for nonlinear Schrödinger equations. *Commun. Theor. Phys.* **68**, 290-294 (2017)
- [6] Zeng, L., Zeng, J.: Gap-type dark localized modes in a Bose-Einstein condensate with optical lattices. *Adv. Photonics* **1**, 046004 (2019)
- [7] Kartashov, Y.V., Astrakharchik, G.E., Malomed, B.A., Torner, L.: Frontiers in multidimensional self-trapping of nonlinear fields and matter. *Nat. Rev. Phys.* **1**, 185-197 (2019)
- [8] Rao, J., He, J., Kanna, T., Mihalache, D.: Nonlocal M-component nonlinear Schrödinger equations: Bright solitons, energy-sharing collisions, and positons. *Phys. Rev. E* **102**, 032201 (2020)
- [9] Wang, Q., Deng, Z.Z.: Controllable propagation path of imaginary value off-axis vortex soliton in nonlocal nonlinear media. *Nonlinear Dyn.* **100**, 1589-1598 (2020)
- [10] Wang Q., Yang, J., Liang, G.: Controllable soliton transition and interaction in nonlocal nonlinear media. *Nonlinear Dyn.* **101**, 1169-1179 (2020)
- [11] Mohebbi, A., Abbaszadeh, M., Dehghan, M.: The use of a meshless technique based on collocation and radial basis functions for solving the time fractional nonlinear Schrödinger equation arising in quantum mechanics. *Eng. Anal. Bound. Elem.* **37**, 475-485 (2013)
- [12] Chan, H.N., Chow, K.W., Kedziora, D.J., Grimshaw, R. H. J., Ding E.: Rogue wave modes for a derivative nonlinear Schrödinger model. *Phys. Rev. E* **89**, 032914 (2014)
- [13] Ao, P., Thouless, D.J., Zhu, X.M.: Nonlinear Schrödinger Equation for Superconductors. *Mod. Phys. Lett. B* **9**, 755-761 (1995)
- [14] Kuznetsov, E.A., Dias, F.: Bifurcations of solitons and their stability. *Phys. Rep.* **507**, 43-105 (2011)
- [15] Christodoulides, D.N., Lederer, F., Silberberg, Y.: Discretizing light behaviour in linear and nonlinear waveguide lattices. *Nature* **424**, 817-823 (2003)
- [16] Morsch O., Oberthaler, M.: Dynamics of Bose-Einstein condensates in optical lattices. *Rev. Mod. Phys.* **78**, 179-215 (2006)
- [17] Garanovich, I.L., Longhi, S., Sukhorukov, A.A., Kivshar, Y.S.: Light propagation and localization in modulated photonic lattices and waveguides. *Phys. Rep.* **518**, 1-79 (2012)
- [18] Kartashov, Y.V., Malomed, B.A., Vysloukh, V.A., Torner, L.: Two-dimensional solitons in nonlinear lattices. *Opt.lett.* **34**, 770-772 (2009)
- [19] Shi, J., Zeng, J.: Self-trapped spatially localized states in combined linear-nonlinear periodic potentials. *Front. Phys.* **15**, 12602 (2020)
- [20] Borovkova, O.V., Kartashov, Y.V., Torner, L., Malomed, B.A.: Bright solitons from defocusing nonlinearities. *Phys. Rev. E* **84**, 035602 (2011)
- [21] Driben, R., Kartashov, Y.V., Malomed, B.A., Meier, T., Torner, L.: Soliton gyroscopes in media with spatially growing repulsive nonlinearity. *Phys. Rev. Lett.* **112**, 020404 (2014)
- [22] Driben, R., Kartashov, Y.V., Malomed, B.A., Meier, T., Torner, L.: Three-dimensional hybrid vortex solitons. *New J. Phys.* **16**, 063035 (2014)
- [23] Zeng, L., Zeng, J., Kartashov, Y.V., Malomed, B.A.: Purely Kerr nonlinear model admitting flat-top solitons. *Opt. Lett.* **44**, 1206-1209 (2019)
- [24] Zeng, L., Zeng, J.: Modulated solitons, soliton and vortex clusters in purely nonlinear defocusing media. *Ann. Phys.* **421**, 168284 (2020)
- [25] Afanasyev, V.V., Kivshar, Y.S., Konotop, V.V., Serkin, V.N.: Dynamics of coupled dark and bright optical solitons. *Opt. Lett.* **14**, 805-807 (1989)
- [26] Chen, Y., Snyder, A.W., Payne, D.N.: Twin core nonlinear couplers with gain and loss. *IEEE J. Quantum Elect.* **28**, 239-245 (1992)
- [27] Litchinitser, N.M., Gabitov, I.R., Maimistov, A.I.: Optical Bistability in a Nonlinear Optical Coupler with a

- Negative Index Channel. Phys. Rev. Lett. **99**, 113902 (2007)
- [28] Chan, H.N., Malomed, B.A., Chow, K.W., Ding, E.: Rogue waves for a system of coupled derivative nonlinear Schrödinger equations. Phys. Rev. E **93**, 012217 (2016)
- [29] Chan, H.N., Chow, K.W.: Rogue wave modes for the coupled nonlinear Schrödinger system with three components: A computational study. Appl. Sci. **7**, 559 (2017)
- [30] Xue, X., Zheng, X., Zhou, B.: Super-efficient temporal solitons in mutually coupled optical cavities. Nat. Photon. **13**, 616-622 (2019)
- [31] Chen, J., Zeng, J.: One-dimensional localized modes of spin-orbit-coupled Bose-Einstein condensates with spatially periodic modulated atom-atom interactions: Nonlinear lattices. Commun. Nonlinear Sci. Numer. Simulat. **85**, 105217 (2020)
- [32] Guo, R., Liu, Y.-F., Hao, H.-Q., Qi, F.-H.: Coherently coupled solitons, breathers and rogue waves for polarized optical waves in an isotropic medium. Nonlinear Dyn. **80**, 1221-1230 (2015)
- [33] Ögren, M., Abdullaev, F.K., Konotop, V.V.: Solitons in a \mathcal{PT} -symmetric $\chi^{(2)}$ coupler. Opt. Lett. **42**, 4079-4082 (2017)
- [34] Zezyulin, D.A., Kartashov, Y.V., Konotop, V.V.: \mathcal{CPT} -symmetric coupler with intermodal dispersion. Opt. Lett. **42**, 1273-1276 (2017)
- [35] Bender, C.M., Boettcher, S.: Real Spectra in Non-Hermitian Hamiltonians Having \mathcal{CPT} -Symmetry. Phys. Rev. Lett. **80**, 5243-5246 (1998)
- [36] Bender, C.M., Boettcher, S., Meisinger, P.N.: \mathcal{PT} -symmetric quantum mechanics. J. Math. Phys. **40**, 2201-2229 (1999)
- [37] Konotop, V.V., Yang, J., Zezyulin, D.A.: Nonlinear waves in \mathcal{PT} -symmetric systems. Rev. Mod. Phys. **88**, 035002 (2016)
- [38] Ramezani, H., Kottos, T., El-Ganainy, R., Christodoulides, D.N.: Unidirectional nonlinear \mathcal{PT} -symmetric optical structures. Phys. Rev. A **82**, 043803 (2010)
- [39] Jing, H., Özdemir, S.K., Lü, X.Y., Zhang, J., Yang, L., Nori, F.: \mathcal{PT} -symmetric phonon laser. Phys. Rev. Lett. **113**, 053604 (2014)
- [40] Wimmer, M., Regensburger, A., Miri, M.A., Bersch, C., Christodoulides, D.N., Peschel, U.: Observation of optical solitons in \mathcal{PT} -symmetric lattices. Nat. Commun. **6**, 7782 (2015)
- [41] Suchkov, S.V., Sukhorukov, A.A., Huang, J., Dmitriev, S.V., Lee, C., Kivshar, Y.S.: Nonlinear switching and solitons in \mathcal{PT} -symmetric photonic systems. Laser Photon. Rev. **10**, 177-213 (2016)
- [42] Huang, M., Lee, R.K., Zhang, L., Fei, S.M., Wu, J.: Simulating broken \mathcal{PT} -symmetric Hamiltonian systems by weak measurement. Phys. Rev. Lett. **123**, 080404 (2019)
- [43] Zhou, H., Lee, J.Y., Liu, S., Zhen, B.: Exceptional surfaces in \mathcal{PT} -symmetric non-Hermitian photonic systems. Optica **6**, 190-193 (2019)
- [44] Klauck, F., Teuber, L., Ornigotti, M., Heinrich, M., Scheel, S., Szameit, A.: Observation of \mathcal{PT} -symmetric quantum interference. Nat. Photon. **13**, 883-887 (2019)
- [45] Herrmann, R.: Fractional Calculus: An Introduction for Physicists. World Scientific, Singapore, (2011)
- [46] Laskin, N.: Fractional quantum mechanics and Lévy path integrals. Phys. Lett. A **268**, 298-305 (2000)
- [47] Laskin, N.: Fractional quantum mechanics. Phys. Rev. E **62**, 3135-3145 (2000)
- [48] Laskin, N.: Fractional Schrödinger equation. Phys. Rev. E **66**, 056108 (2002).
- [49] Stickler, B.A.: Potential condensed-matter realization of space-fractional quantum mechanics: The one-dimensional Lévy crystal. Phys. Rev. E **88**, 012120 (2013)
- [50] Longhi, S.: Fractional Schrödinger equation in optics. Opt. Lett. **40**, 1117-1120 (2015)
- [51] Zhang, Y., Liu, X., Belić, M.R., Zhong, W., Zhang, Y., Xiao, M.: Propagation dynamics of a light beam in a fractional Schrödinger equation. Phys. Rev. Lett. **115**, 180403 (2015)
- [52] Zhang, L., Li, C., Zhong, H., Xu, C., Lei, D., Li, Y., Fan, D.: Propagation dynamics of super-Gaussian beams in fractional Schrödinger equation: From linear to nonlinear regimes. Opt. Express **24**, 14406-14418 (2016)
- [53] Zhang, Y., Zhong, H., Belić, M.R., Ahmed, N., Zhang, Y., Xiao, M.: Diffraction-free beams in fractional Schrödinger equation. Sci. Rep. **6**, 23645 (2016)
- [54] Zhang, Y., Zhong, H., Belić, M.R., Zhu, Y., Zhong, W., Zhang, Y., Christodoulides, D.N., Xiao, M.: \mathcal{PT} -symmetry in a fractional Schrödinger equation. Laser Photon. Rev. **10**, 526-531 (2016)
- [55] Zhong, W.P., Belić, M.R., Malomed, B.A., Zhang, Y., Huang, T.: Spatiotemporal accessible solitons in fractional dimensions. Phys. Rev. E **94**, 012216 (2016)
- [56] Zhong, W.P., Belić, M.R., Zhang, Y.: Accessible solitons of fractional dimension. Ann. Phys. **368**, 110-116 (2016)
- [57] Huang, C., Dong, L.: Gap solitons in the nonlinear fractional Schrödinger equation with an optical lattice. Opt. Lett. **41**, 5636-5639 (2016)
- [58] Zhang, Y., Wang, R., Zhong, H., Zhang, J., Belić, M.R., Zhang, Y.: Optical Bloch oscillation and Zener tunneling in the fractional Schrödinger equation. Sci. Rep. **7**, 17872 (2017)
- [59] Zhang, L., He, Z., Conti, C., Wang, Z., Hu, Y., Lei, D., Li, Y., Fan, D.: Modulational instability in fractional nonlinear Schrödinger equation. Commun. Nonlinear Sci. Numer. Simulat. **48**, 531-540 (2017)
- [60] Zhang, Y., Wang, R., Zhong, H., Zhang, J., Belić, M.R., Zhang, Y.: Resonant mode conversions and Rabi oscillations in a fractional Schrödinger equation. Opt. Express **25**, 32401-32410 (2017)
- [61] Wang, Q., Li, J., Zhang, L., W, Xie.: Hermite-gaussian-like soliton in the nonlocal nonlinear fractional Schrödinger equation. EPL **122**, 64001 (2018)
- [62] Yao, X., Liu, X.: Off-site and on-site vortex solitons in space-fractional photonic lattices. Opt. Lett. **43**, 5749-5752 (2018)
- [63] Wang, Q., Deng Z.Z.: Elliptic Solitons in (1+2)-Dimensional Anisotropic Nonlocal Nonlinear Fractional Schrödinger Equation. IEEE Photonics J. **11**, 1-8 (2019)
- [64] Zeng, L., Zeng, J.: One-dimensional solitons in fractional Schrödinger equation with a spatially periodical modulated nonlinearity: nonlinear lattice. Opt. Lett. **44**, 2661-2664 (2019)
- [65] Xie, J., Zhu, X., He, Y.: Vector solitons in nonlinear fractional Schrödinger equations with parity-time-symmetric optical lattices. Nonlinear Dyn. **97**, 1287-1294 (2019)
- [66] Li, P., Li, J., Han, B., Ma, H., Mihalache, D.: \mathcal{PT} -symmetric optical modes and spontaneous symmetry breaking in the space-fractional Schrödinger equation. Rom. Rep. Phys. **71**, 106 (2019).

- [67] Zeng, L., Zeng, J.: One-dimensional gap solitons in quintic and cubic-quintic fractional nonlinear Schrödinger equations with a periodically modulated linear potential. *Nonlinear Dyn.* **98**, 985-995 (2019)
- [68] Zhang, L., Zhang, X., Wu, H., Li, C., Pierangeli, D., Gao, Y., Fan, D.: Anomalous interaction of Airy beams in the fractional nonlinear Schrödinger equation. *Opt. Express* **27**, 27936-27945 (2019)
- [69] Dong, L., Huang, C.: Vortex solitons in fractional systems with partially parity-time-symmetric azimuthal potentials. *Nonlinear Dyn.* **98**, 1019-1028 (2019)
- [70] Zeng, L., Zeng, J.: Preventing critical collapse of higher-order solitons by tailoring unconventional optical diffraction and nonlinearities. *Commun. Phys.* **3**, 26 (2020)
- [71] Li, P., Malomed, B.A., Mihalache, D.: Metastable soliton necklaces supported by fractional diffraction and competing nonlinearities. *Opt. Express* **28**, 34472-34488 (2020)
- [72] Wang, Q., Liang, G.: Vortex and cluster solitons in non-local nonlinear fractional Schrödinger equation. *J. Optics* **22**, 055501 (2020)
- [73] Chen, J., Zeng, J.: Spontaneous symmetry breaking in purely nonlinear fractional systems. *Chaos* **30**, 063131 (2020)
- [74] Zeng, L., Zeng, J.: Fractional quantum couplers. *Chaos Soliton Fract.* **140**, 110271 (2020)
- [75] Shi, J., Zeng, J.: 1D Solitons in Saturable Nonlinear Media with Space Fractional Derivatives. *Ann. Phys. (Berlin)* **532**, 1900385 (2020)
- [76] Zhu, X., Yang, F., Cao, S., Xie, J., He, Y.: Multipole gap solitons in fractional Schrödinger equation with parity-time-symmetric optical lattices. *Opt. Express* **28**, 1631-1639 (2020)
- [77] Li, P., Dai, C.: Double Loops and Pitchfork Symmetry Breaking Bifurcations of Optical Solitons in Nonlinear Fractional Schrödinger Equation with Competing Cubic-Quintic Nonlinearities. *Ann. Phys. (Berlin)* **532**, 2000048 (2020)
- [78] Qiu, Y., Malomed, B.A., Mihalache, D., Zhu, X., Zhang, L., He, Y.: Soliton dynamics in a fractional complex Ginzburg-Landau model. *Chaos Soliton Fract.* **131**, 109471 (2020)
- [79] Li, P., Malomed, B.A., Mihalache, D.: Symmetry breaking of spatial Kerr solitons in fractional dimension. *Chaos Soliton Fract.* **132**, 109602 (2020)
- [80] Li, P., Malomed, B.A., Mihalache, D.: Vortex solitons in fractional nonlinear Schrödinger equation with the cubic-quintic nonlinearity. *Chaos Soliton Fract.* **137**, 109783 (2020)
- [81] Qiu, Y., Malomed, B.A., Mihalache, D., Zhu, X., Peng, X., He, Y.: Stabilization of single- and multi-peak solitons in the fractional nonlinear Schrödinger equation with a trapping potential. *Chaos Soliton Fract.* **140**, 110222 (2020)
- [82] Kivshar, Y.S., Luther-Davies, B.: Dark optical solitons: physics and applications. *Phys. Rep.* **298**, 81-197 (1998)
- [83] Yang, J.: *Nonlinear Waves in Integrable and Nonintegrable Systems*, SIAM, Philadelphia, (2010)
- [84] Vakhitov, N.G., Kolokolov, A.A.: Stationary solutions of the wave equation in a medium with nonlinearity saturation. *Radiophys. Quantum Electron.* **16**, 783-789 (1973)
- [85] Kartashov, Y.V., Konotop, V.V., Abdullaev, F.K.: Gap solitons in a spin-orbit-coupled Bose-Einstein condensate. *Phys. Rev. Lett.* **111**, 060402 (2013)